DOI: 10.13009/EUCASS2019-357

Preparation, evaluation and characterization of catalytic beds for a trigas chemical propulsion thruster

Pierre Chabernaud[1,2], Romain Beauchet[1], Yann Batonneau[1], Charles Kappenstein[1], Marie-Thérèse Prodhomme[2], Ulrich Gotzig[3], Jean-Philippe Dutheil[4]

[1]IC2MP – 4 rue Michel Brunet, 86000 Poitiers, France

yann.batonneau@univ-poitiers.fr

[2]ArianeGroup – 51-61 Route de Verneuil, 78133 Les Mureaux, France

[3]ArianeGroup – Langer Grund, 74239 Hardthausen, Germany

[4]ArianeGroup – rue du Gl Niox, Issac, 33165 Saint-Médard-en-Jalles, France

Abstract

Cold gas propulsion is the simplest propulsion technology with the advantage of being a simple and safe system, but the disadvantages that it's I_{SP} and storage density are limited compared to classical chemical propulsion systems. By adding a controlled amount of combustible gases, it can be transferred to a "warm gas" system with increased performances. The present work considers alternatives to current operational cold gas propulsion systems. Trigas systems meet these requirements for both small satellite propulsion and Space Plane application. The implementation of a catalytic chamber demonstrates high performances. Promising results were obtained with various platinum-based catalysts.

1. Introduction

Cold gas propulsion technology consists in releasing pressurized inert gas (mostly nitrogen N_2) through a nozzle to generate thrust. The inevitable drawbacks of this system are substantial temperature drops induced by the gas expansion, leading to a loss of specific impulse (I_{SP} = 75-80 s).
To overcome this problem, trigas technology can be considered. The first works were performed by Rocketdyne in the 1960s [1].
The main advantages are that it remains a "green" technology, is lighter in terms of mass and volume and has the potential to have better performances. It could be applicable to small satellite propulsion or SpacePlane.
Trigas relies on the generation of thrust from a pressurized gas mixture heated through the catalytic combustion of one of the constituents of the mixture. It is based on three (or more) gas components:

- A fuel: H_2
- An oxidizer: O_2
- A diluent (or a mixture of diluting gases): N_2, Ar, He [2], CO_2, etc.

The diluent can be "inert", *i. e.* not contributing to the catalytic combustion of hydrogen. Fuel and oxidizer are added in such proportions that they do not react with each other, unless the reaction be triggered.
The hydrogen combustion reaction has been known since the beginning of the 19th century and has since then been addressed by numerous experimental and theoretical studies. Kinetic studies have been conducted by Boreskov *et al.* on this reaction catalyzed by metals (Fe, Co, Cu, Pt, Pd, Rh, Au and Ag) [3]. They showed that metals with a complete electronic d-sublayer exhibited better catalytic activity for the chain reaction mechanism. Platinum for instance displayed promising results for the catalytic hydrogen catalytic combustion in hydrogen-air mixtures [4], and for cryogenic hydrogen-oxygen ignitions as well [5].
The first need of the study was to select at least one trigas composition in order to be safe in terms of use and storage, while being interesting in a performance aspect, *i. e.* improving the specific impulse compared to cold gas.

Thus, a mixture of 10 % (v/v) H_2, 5 % (v/v) O_2 and 85 % (v/v) N_2 has been established as the reference composition. The choice was mainly based on the work of Rigas and Amyotte [6] in which this composition appears in the non-flammable region at ambient temperature and atmospheric pressure.

DOI: 10.13009/EUCASS2019-357

The mixture was flown through a catalytic bed to deliver heat released by hydrogen combustion. The catalyst substrate consisted of a monolithic structure with straight square channels. It was washcoated with a porous material on which an active phase was dispersed. The nature of the active phase was a noble metal, namely either platinum or rhodium. The evaluation of the catalytic performance was performed on a test bench. Pre-testing and post-testing physicochemical characterizations were also performed to find connections between performance results and catalyst structure and characteristics: X-Ray Diffraction, Transmission- and Scanning Electron Microscopy, and nitrogen sorptiometry.

2. Experimental section

2.1 Choice of the catalytic structure

Catalysts supported on monolithic structures display interesting performances for various applications, especially for the automotive industry, where it has been widely studied during the past years [7]. They present interesting aspects, useful for high temperature applications: it is lighter in terms of mass, presents a lower back pressure than regular pelleted catalysts, and it also limits attrition as can be experienced with pellets [8]. Their main drawbacks are low flow turbulence (essentially caused by straight channels), and fragility of the structure, compared to pellets.

In this work, a high density square channels (600 cells per square inch, cpsi) monolith was chosen to favour the contact between the reactive gas and the active phase. The material nature was cordierite which ensured thermal resistivity with the temperatures expected with this trigas technology.

2.2 Catalyst preparation

Ceramic block of cordierite ($2MgO{\cdot}2Al_2O_3{\cdot}5SiO_2$ length (L): 102 mm; diameter (Ø): 143 mm) was provided by CTISA, Salindres, France. It was cut to the desired dimension (L: 20 mm; Ø: 10 mm) using a hole-saw (diameter) and a diamond wire (length). Both the block and a typical piece thus obtained are displayed in Figure 1.

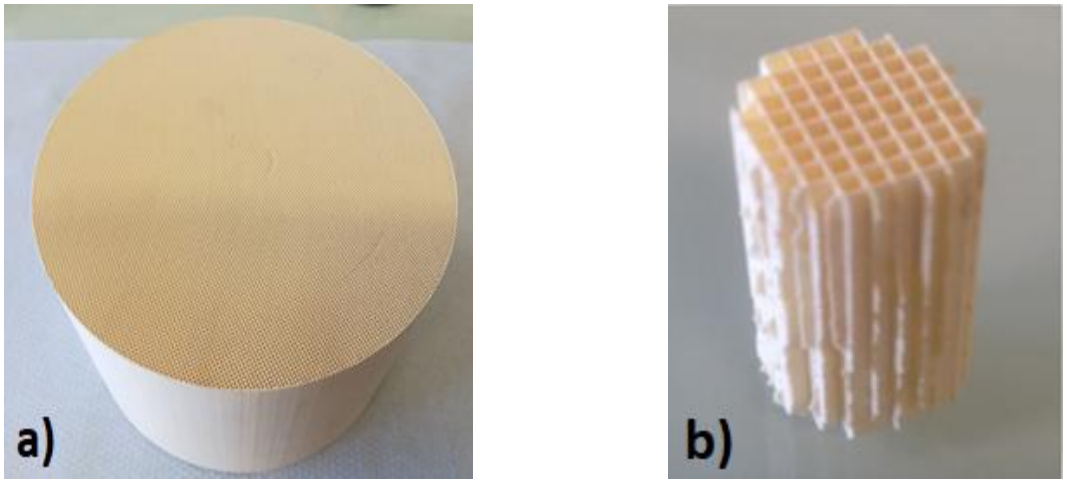

Figure 1: a) Ceramic block as received (Ø 143 mm) and b) after cutting (Ø 10 mm)

Carrier pieces cut were coated with a high specific surface area material, since cordierite has a good porosity (*ca* 35 %) but a low specific surface area (< 0.5 $m^2\ g^{-1}$).

For that, the carrier was washed in concentrated nitric acid for two hours, then rinsed, dried, and finally subjected to a specific thermal treatment. Then, alumina was synthesised via a sol-gel method, from a specific aluminium precursor (SASOL boehmite dispersal P2). The coating step of the monolith carriers consisted in immersing them into the colloidal solution for a controlled time, and then unclog the potential alumina surplus with an argon flow. An important aspect of the coating step was the control of the colloidal solution viscosity, which was done after the sol synthesis.

Then, the coated monoliths were subjected to a thermal treatment at 500 °C in a muffle furnace to dry the coating phase.

DOI: 10.13009/EUCASS2019-357

After this, the coated monoliths were impregnated (deposition of the active phase onto the surface) thanks to the wet-impregnation method. The method consisted in immersing the monolith in a solution containing an active phase precursor under orbital agitation. After this step, the excess of the solution was dried and evaporated in a sand bath at 65 °C for at least ten hours. The catalysts were then dried at 120 °C for one hour. Thermal treatments depending on the nature of the active phase deposited on the catalyst surface were finally performed.

The catalyst aspect is photographed in Figure 2 after each preparation step.

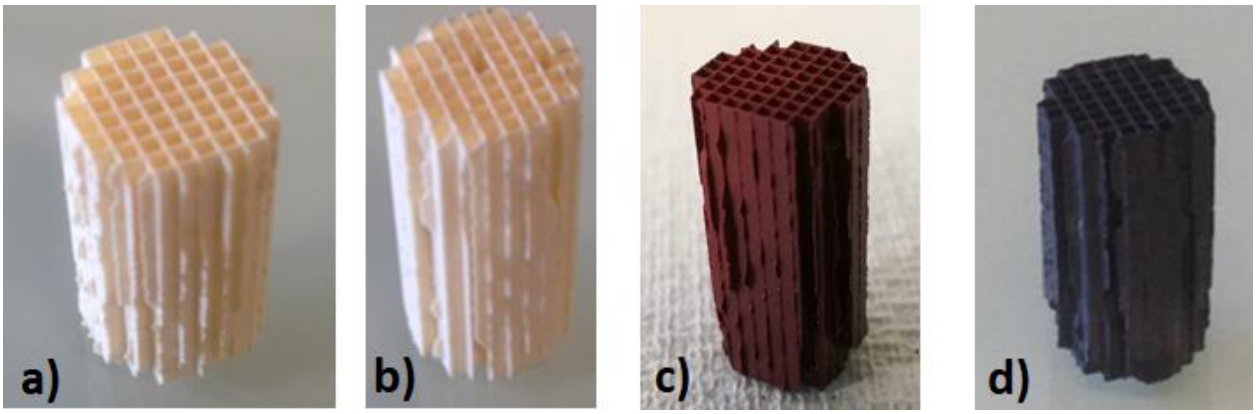

Figure 2 Catalysts views along the preparation steps. a) raw monolith; b) coated monolith; c) impregnated monolith; d) catalyst after final thermal treatment

Catalysts were weighed after each preparation step.

2.3 Laboratory-scale test bench

The bench used for tests is presented in Figure 3. The trigas mixture was generated from pressurized cylinders of individual constituents, one for H_2, one for O_2 and another one for N_2, using mass flowrate controllers. The gases were mixed (see point 5 in Figure 3), flow inside a cooling tank which can regulate temperatures down to -80 °C. A three-way valve at the outlet of the cooling tank enabled switching to venting or through the chamber in which the catalyst is loaded. A micro-gas chromatograph (Agilent µ-GC 490) located at the outlet of the reactor allowed the quantitative estimation of non-reacting gases.

DOI: 10.13009/EUCASS2019-357

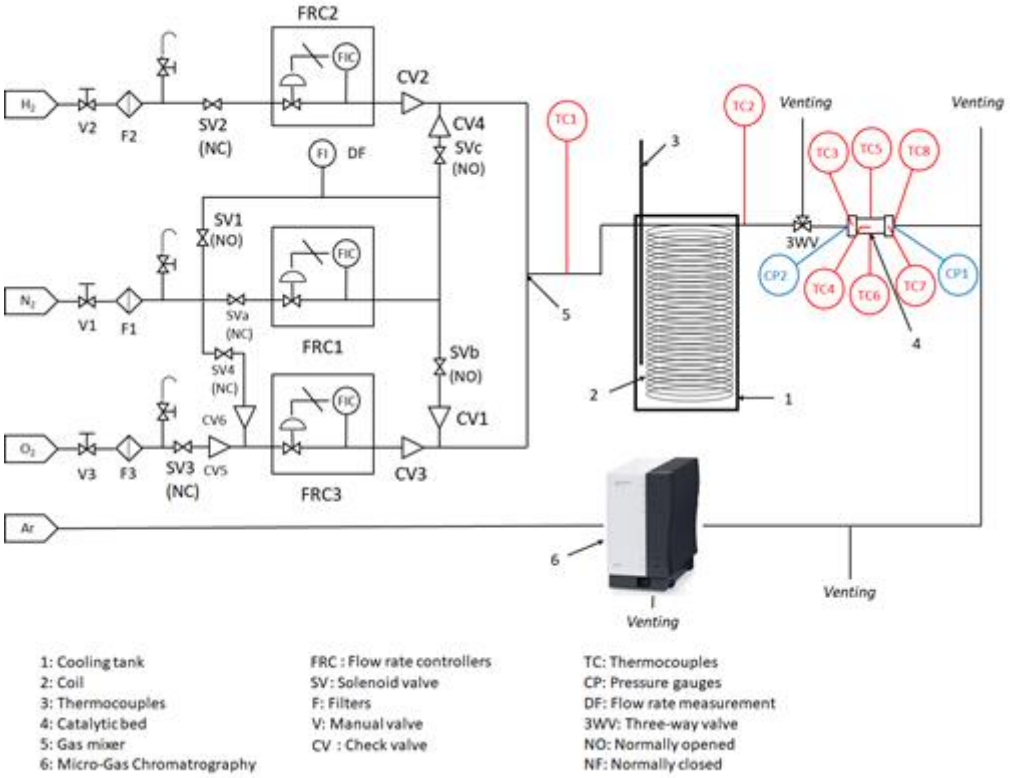

Figure 3: Schematic view of the test bench

The tubing was Ø 1/4”, 316L stainless steel (Swagelok). A Ø 1/8” 316L stainless steel (Swagelok) pipe was used to feed the gas-chromatograph. The chamber used for catalytic tests had an internal diameter of 10 mm and was 20 mm long. It is photographed in Figure 4. The positions of the thermocouples (Ø 0.5 mm) are given in Figure 4.

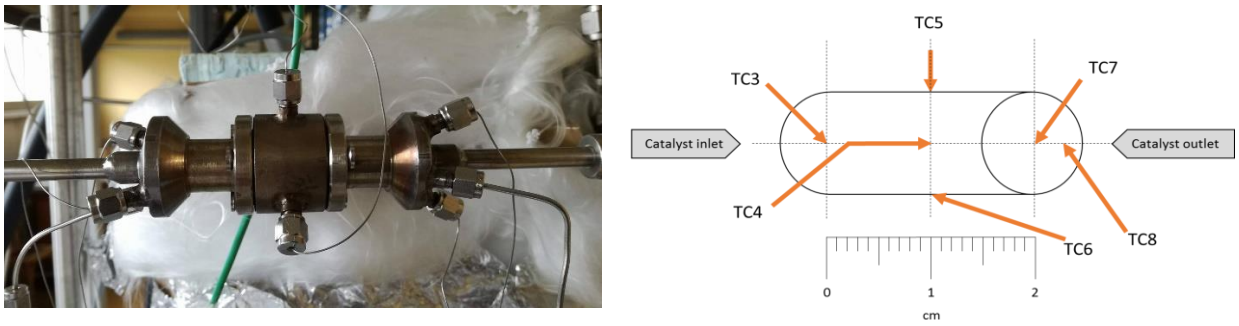

Figure 4: Picture (left) and schematic view (right) of the catalytic chamber with the positioning of the thermocouples (right)

Thermocouple TC5 was so positioned that the temperature at the edge of the internal wall of the chamber could be recorded. Thermocouple TC6 was positioned in the middle of the chamber wall thickness. TC3, TC4, TC7 and TC8 measure the fluid temperature at different locations in the reactor.

The test sequence for each catalytic combustion test was as follows: the set-up was purged with gaseous nitrogen for several minutes. Then hydrogen was flown at the required mass flowrate mixed with nitrogen. A third step began when oxygen was flown into the set-up as well. The trigas mixture thus obtained by-passed the reactor thanks to the three-way valve. The fourth step consisted in switching the three-way valve to the catalytic chamber, so that the gases could contact the catalyst, leading to eventual combustion. Finally, a fifth step was added at the end of the combustion step where the gaseous nitrogen flows for several reasons: first it evacuates the remaining combustion gases, and it also cools down the chamber. For the needs of the study, catalytic combustion tests were conducted between -55 °C and the ambient temperature to evaluate the catalysts performances, the gas composition being invariant.

DOI: 10.13009/EUCASS2019-357

The test sequence is reminded in Table 1.

Table 1: Description of a combustion test sequence

Step # → action	Nature of gas flowing / gas pathway / typical duration
1 → Remaining gases reactor purging	N_2 / reactor / 20 s
2 → Hydrogen and nitrogen mixing for flow stabilization	$N_2 + H_2$ / venting / 10 to 20 s
3 → Hydrogen, oxygen and nitrogen mixing for flow stabilization	$N_2 + H_2 + O_2$ / venting / 10 s
3bis → Combustion step with the trigas mixture	$N_2 + H_2 + O_2$ / reactor / 20 to 90 s
4 → Remaining gases piping purging	N_2 / venting / 10 s

The time for each step can be adjusted depending upon the test needs, though the same sequence was used for a better comparison between catalysts, flows, and initial temperatures, for most of the tests performed.

Temperature, pressure, mass flowrate, and phase steps signals were acquired and recorded during the test using a FLUKE data acquisition piloted using a Labview program. Figure 5 displays typical signals thus obtained.

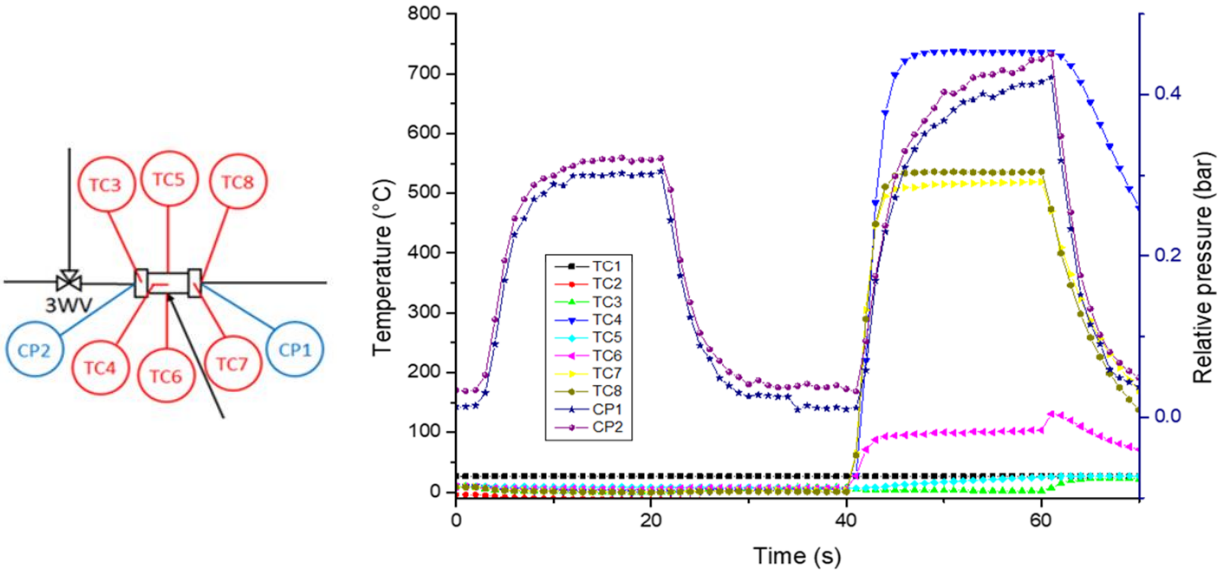

Figure 5: Typical temperature and pressure signals recorded during combustion tests. The drawing on the left reminds the position and codes of the temperature (TC) and pressure (CP) sensors

Figure 5 exemplifies a result of a so-called continuous mode test, whereby the reacting gases are flown through the catalytic chamber only once for 20 s. The different steps could be modulated by cumulating successive combustion steps for shorter durations thanks to the three-way valve, which time response is about 50 ms. The so-called tests are called pulse mode tests. Figure 6 displays typical signals thus obtained.

DOI: 10.13009/EUCASS2019-357

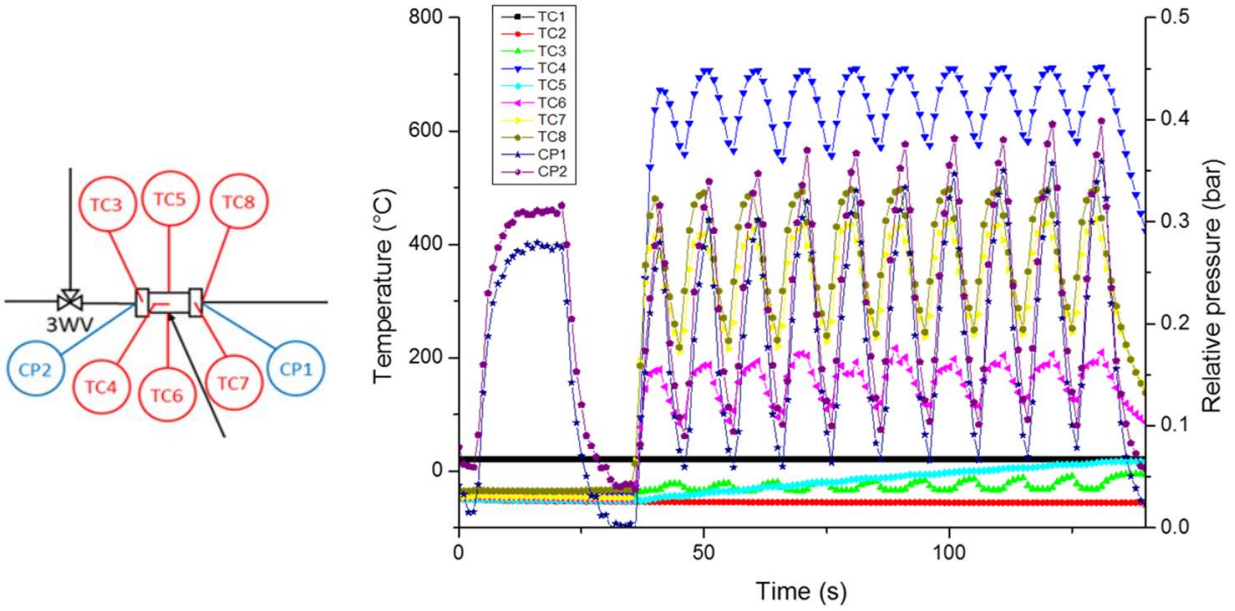

Figure 6: Typical test profile in pulse mode (10 pulses, 5 s valve opening per pulse)

The temperature increases between 40 s and 60 s (corresponding to the fourth step in Figure 5) and between 40 s and 130 s (Figure 6) indicate, here, that the catalyst ignited the mixture in both steady-state and pulse modes.

3. Results and discussion

3.1 Prepared catalysts

Catalysts were prepared following the procedure described in section 2.2. The substrates dimensions were measured using a caliper, they were about 9.84 ± 0.15 mm in diameter and 20.05 ± 0.13 mm in length. The coating procedure (deposition of γ-Al_2O_3) was so implemented that the porous layer reached 15 % in mass of the washcoated monolith one. Several catalysts have been prepared with different active phases at different mass loadings and have been tested on the test bench. For each composition, three catalysts were prepared following the same procedure. Platinum-based and rhodium-based catalysts (from 0.08 % w.t to 30 % w.t) were elaborated for this study.

3.2 Catalysts performance evaluation

Initial temperatures considered for tests were: -55 °C; -30 °C; -10 °C and ambient temperature.

The gas flowrates were limited by the flowmeter specifications and range (NL stands for normal litre at 298 K and 1 atm):

- N_2: from 0 to 250 NL min^{-1} (0 to 4.8 g s^{-1})
- H_2: from 0 to 25 NL min^{-1} (0 to $3.4 \cdot 10^{-3}$ g s^{-1})
- O_2: from 0 to 25 NL min^{-1} (0 to 0.5 g s^{-1})

Tests were performed from 0.09 g s^{-1} to 3.50 g s^{-1} for steady-state tests and from 0.09 g s^{-1} to 0.90 g s^{-1} for pulse-mode tests.

These first parameters allowed the authors to conduct an ignition feasibility study for a given catalytic system at laboratory level.

To assess the catalyst efficiency, several parameters were considered: T_{ini} (combustion test initial temperature) determined from TC3; T_{max} (maximum temperature recorded during the combustion test) with TC7. ΔT is the difference between T_{max} and T_{ini}; s_T is the temperature variation slope determined during the combustion test; Δt is the corresponding time duration. These parameters and the way they are determined are described in Figure *7*.

DOI: 10.13009/EUCASS2019-357

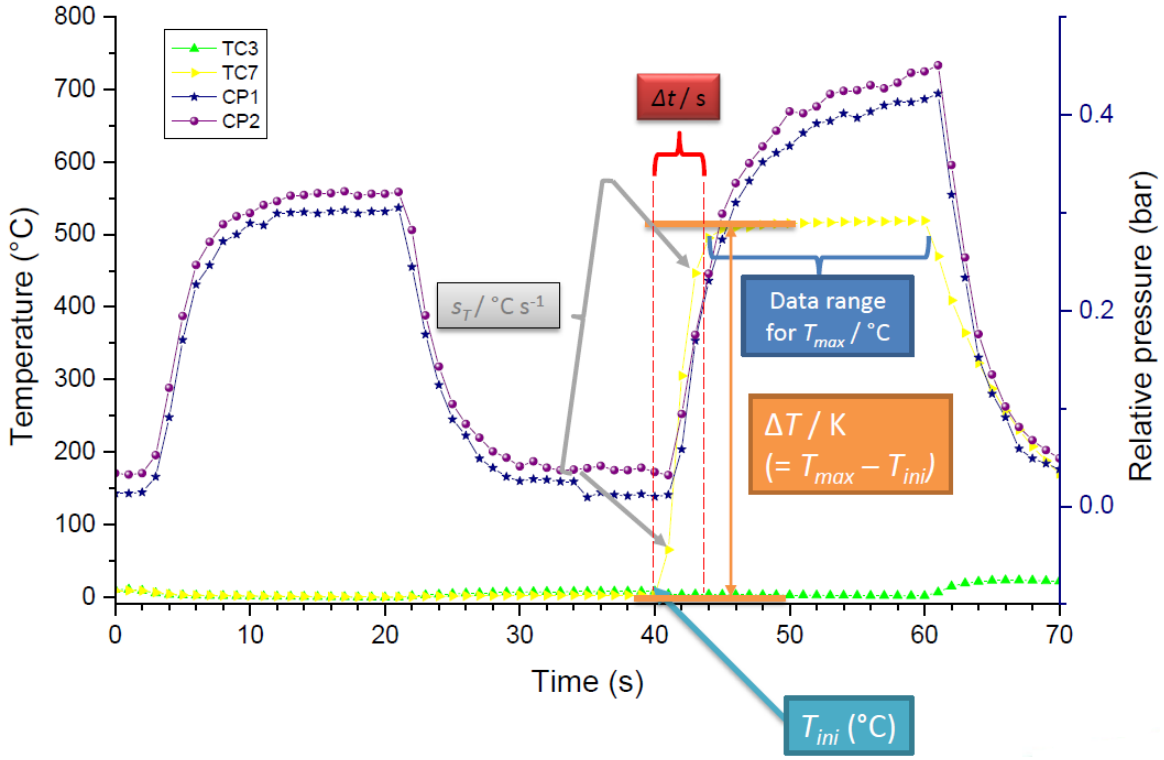

Figure 7: Key parameters presentation for the catalyst efficiency estimation. TC3 and 7 are signals obtained from thermocouples, CP1 and 2, from pressure gauges (see *e. g.* Figure 6)

The T_{max} values, and thus the s_T values, obtained during tests were different according to the amount of gas flowing inside the catalytic reactor. These values are presented in Table 2 for a 5 % Pt catalyst at T_{ini} = ambient temperature.

Table 2: T_{max} and s_T values for a 5 % Pt catalysts for tests at ambient temperature

Total flowrate (NL min^{-1} / g s^{-1})	**T_{max} / °C**	**s_T / °C s^{-1}**
5 / 0.09	421	36
7 / 0.12	497	50
8 / 0.14	536	65
10 / 0.17	524	77
15 / 0.26	609	106
25 / 0.44	593	146
40 / 0.70	616	124
50 / 0.87	530	180
60 / 1.05	511	146
70 / 1.22	496	146
80 / 1.40	476	195
90 / 1.57	479	173
100 / 1.74	369	111
110 / 1.92	429	178
150 / 2.62	288	117

For the catalytic performance evaluation and design, another parameter was considered: the GHSV (Gas Hourly Space Velocity). It is defined in equation (1):

$$GHSV = \frac{\dot{V}_{gas}}{V_{cata}} \quad \textbf{(1)}$$

DOI: 10.13009/EUCASS2019-357

GHSV (in min^{-1}) is a function of $\dot{V}_{gas}$ (total volumetric flow in L min^{-1}) and V_{cata} (catalytic bed volume in L), it indicates how many volumes of gaseous mixture feed one unit of catalytic bed volume and per unit of time. It is adequate to optimize catalytic bed dimensions.
By keeping the same catalyst volume and varying the total volumetric flow, different tests can be performed to try to find the optimum GHSV based upon a maximum ΔT (see section 2.3).
An example of the optimum GHSV determination with a 5 % Pt catalyst is shown in Figure 8.

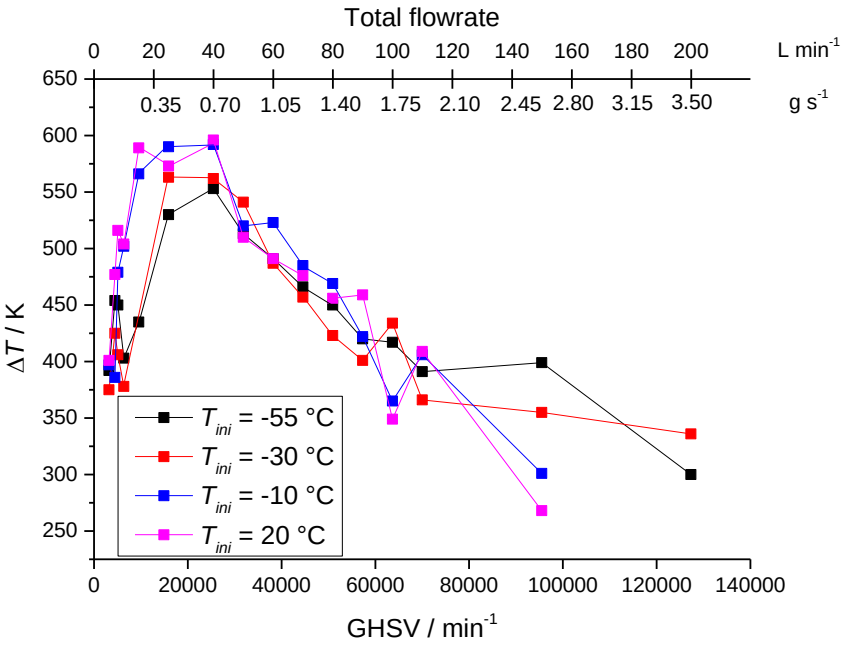

Figure 8: Examples of ΔT recordings as a function of GHSV with a 5 % Pt catalyst at different initial temperatures (T_{ini})

The optimum GHSV lies in the 20,000-30,000 min^{-1} range, and this, for all initial temperatures considered. This means that the system will be operational at any initial temperature, and will be efficient at the same GHSV. This assessment will be of great help for future catalytic bed upscaling. The results obtained though have to be confirmed by tests at higher scale in terms of dimensioning before the assessment at 1:1 scale.

The other aspect of the study was to optimize the active phase loading, keeping good performances, to lower the overall cost of catalyst manufacture and to rationalise the consumption of metals. For this, platinum-based catalysts were prepared with lower percentages of active phase. Test results obtained at T_{ini} = 20 °C are compared with the one obtained with the 5 % Pt catalyst in Figure 9.

DOI: 10.13009/EUCASS2019-357

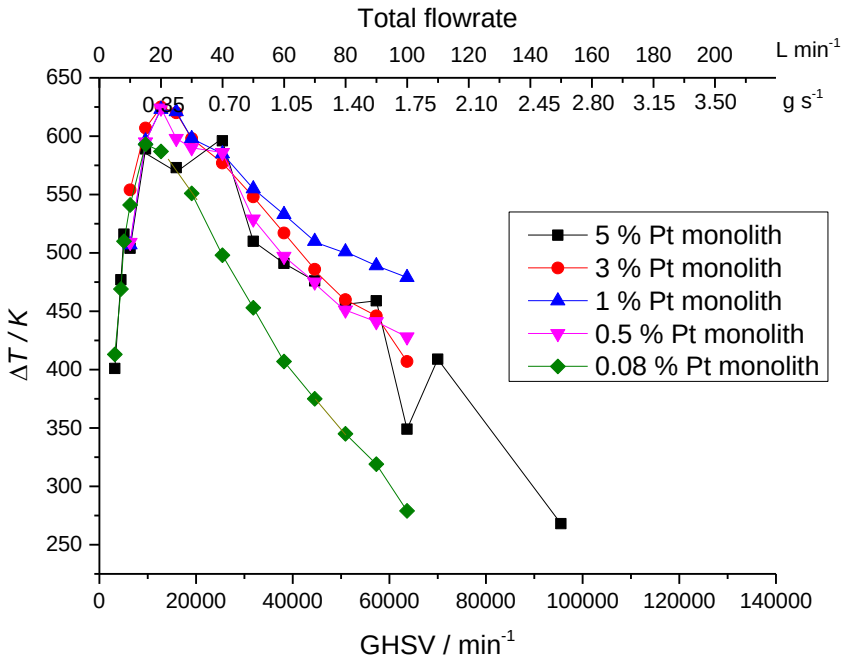

Figure 9: Δ*T* recordings as a function of GHSV with various platinum loadings at 20 °C

Despite the poorer performances exhibited by the least platinum mass deposit catalyst (0.08 %), the performances are comparable between the other ones. Tests were performed at other initial temperatures, what led to similar conclusions.

Even though TC7 was used to determine the performances of the catalysts to better assess the specific impulse of the system, the highest temperatures reached were recorded in the middle of the reactor (TC4) for all tests. This could pave the way to a possible catalytic bed re-dimensioning consisting in reducing the length of the catalyst. This could allow to reach better performances, because the higher temperature recorded in the middle of the reactor could indicate that the second half of the monolith is not necessary.
Estimations were made concerning thrust and specific impulse performances based on the results obtained on the 5 % Pt catalyst, thanks to equations (2) to (5).

$$C_{fvacuum} = \left[\left(\frac{2\gamma^2}{\gamma-1}\right).\left(\frac{2}{\gamma+1}\right)^{\frac{\gamma+1}{\gamma-1}}.\left(1-\left(\frac{P_e}{P_c}\right)^{\frac{\gamma-1}{\gamma}}\right)\right]^{\frac{1}{2}} + \frac{S_e P_e}{S_t P_c} \quad \textbf{(2)}$$

$$C^* = \left(\frac{\gamma+1}{2}\right)^{\frac{(\gamma+1)}{2(\gamma-1)}}\left[\frac{R\,T}{\gamma\,MM}\right]^{\frac{1}{2}} \quad \textbf{(3)}$$

$$I_{SP} = \frac{C_{fvacuum}C^*}{g_o} \quad \textbf{(4)}$$

$$F = qC_{fvacuum}C^* \quad \textbf{(5)}$$

$C_{fvacuum}$ is the thrust coefficient in vacuum conditions, it depends only on nozzle characteristics (except for γ). The expression can be simplified to the first-two terms between the hooks since the calculations are done for a P_e value of zero. C^* is the characteristic exhaust velocity and focus on the propellant and chamber performance. Thus, the thrust (F) and specific impulse values could be determined for the catalytic system used at different flowrates, as it is studied in Figure 10.

DOI: 10.13009/EUCASS2019-357

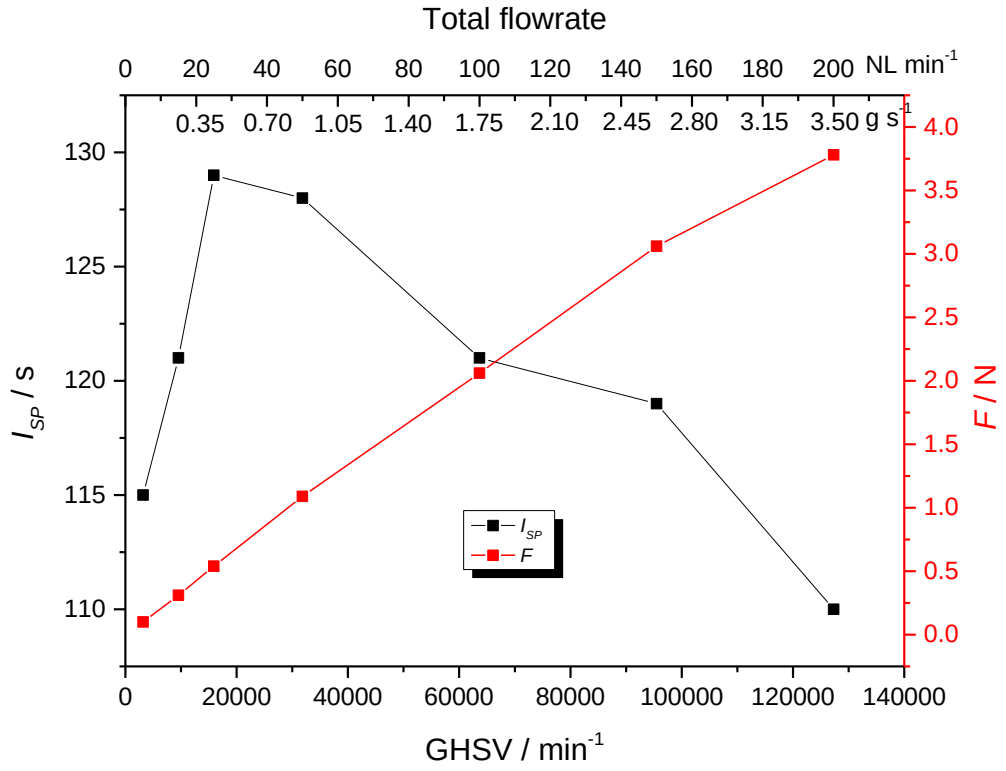

Figure 10: Specific impulse and thrust values determined with a 5 % Pt catalyst

The Figure above highlights the system capacity in terms of thrust performances, where a theoretical thrust of 3.8 N could be reached at the highest flowrates. A significant I_{SP} improvement was proved (up to 130 s), when compared to cold gas technology (75-80 s).

The µ-GC situated at the reactor outlet (see section 2.3) allows a quantitative (and qualitative) analysis of gases at the the reactor outlet. This has been used to monitor the presence or not of remaining hydrogen and oxygen during the combustion step. The absence of these gases would mean that they were fully converted into water. In such conditions, the catalyst would be considered as fully efficient.
Some preliminary results were obtained with platinum-based catalysts: at lower flowrates hydrogen and oxygen could not be seen with the µ-GC. However, with the increase of the total flowrates, remaining reactive gases were measured and their concentration increased with the trigas flowrate, as seen in Figure 11, where the percentage of remaining gases is compared to the ΔT recording for a 3 % Pt monolith catalyst.

DOI: 10.13009/EUCASS2019-357

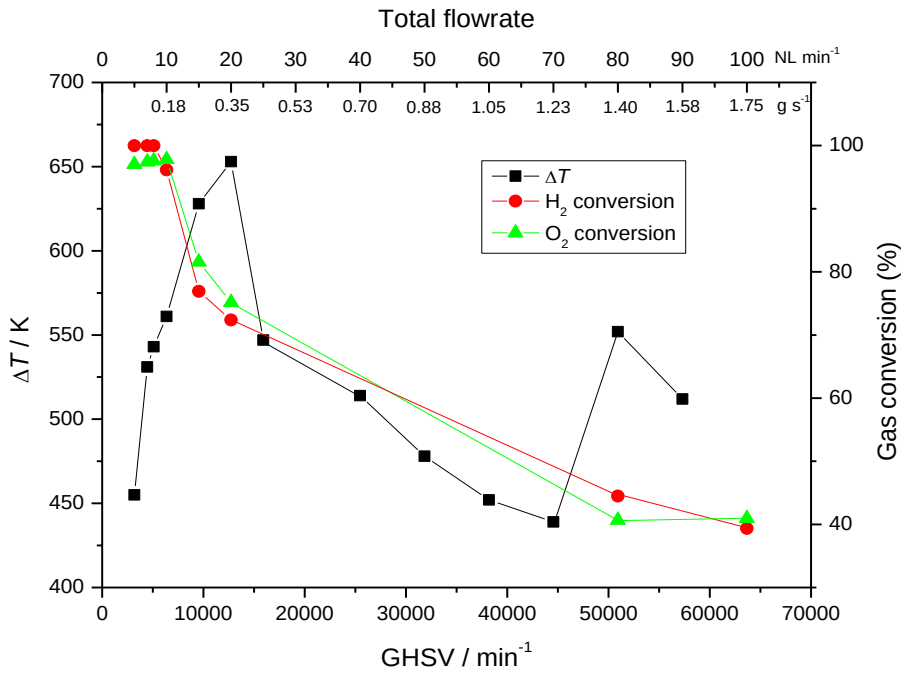

Figure 11: Remaining gases quantification with relation of recorded ΔT for a 3 % Pt catalyst

Some hypotheses could be made about this behaviour: at lower flowrates, reactive gases are consumed but the heat generation is not enough sufficient to increase the temperature of the system. At higher flowrates (above a GHSV of 8000 min^{-1}), some H_2 and O_2 is not converted, indicating that all active sites are already busy and are not able anymore to have all the H_2 and O_2 molecules reacted into water. Despite this, the highest temperatures are recorded at around 20,000 min^{-1} GHSV. This shows that at these flowrates, even though the reactive gases are not fully converted, the amount of gas burnt releases more heat than at lower flowrates.

Several catalysts (mostly rhodium-based catalysts) displayed interesting behaviours during the combustion tests: they needed a preliminary combustion at lower flowrates in order to get a successful ignition at higher flowrates, as depicted in Table 3.

Table 3: Test sequence for a 15 % Rh catalyst at ambient temperature and its ability to ignite the mixture (grey spots = N/A)

Test sequence / Flow (g s^{-1})	1	2	3	4	5	6	7	8	9	10
0.17						Ignition				
0.26					Ignition					
0.34				No ignition			Ignition			
0.88	No ignition							Ignition		
1.75		No ignition							Ignition	
2.62			No ignition							Ignition

DOI: 10.13009/EUCASS2019-357

Several assumptions could be made for this “pre-activation” process: (i) partial removal of chlorine from the catalyst which inhibited the performances; (ii) decrease of humidity adsorption poisoning the active phase; (iii) metal dispersion modification.
To answer these questions, physicochemical characterizations of the catalysts were undertaken.

3.3 Catalysts characterization

- Scanning electron microscopy (SEM)

SEM technique was used to observe the deposition of γ-alumina on the surface of the catalyst carrier. Two SEM images of a monolithic carrier before and after washcoating are displayed in Figure 12.

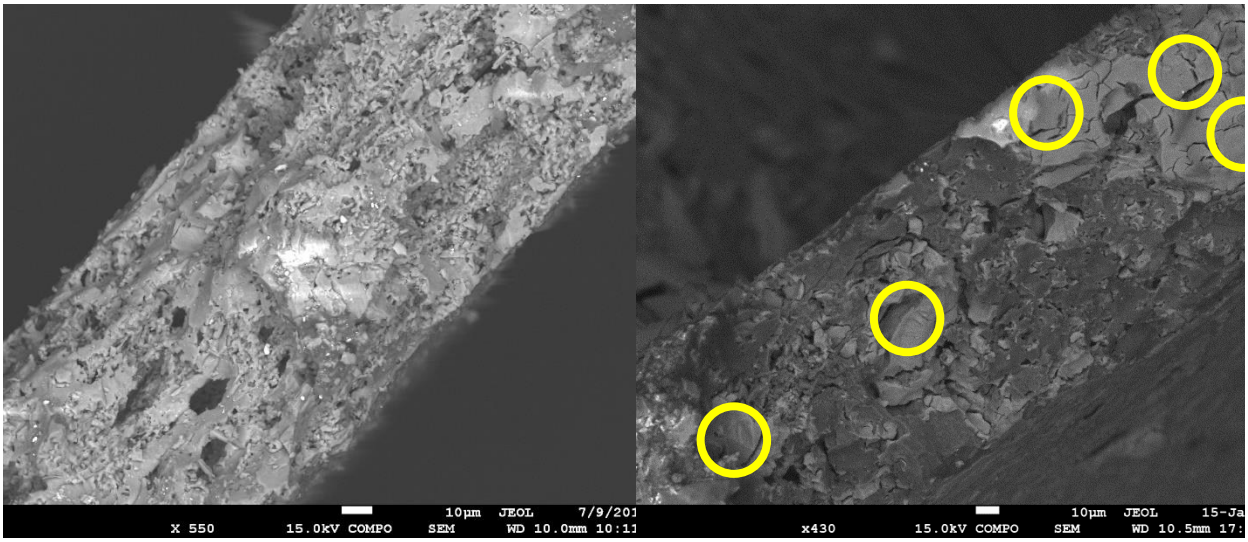

Figure 12: SEM clichés of a cordierite monolith channel without alumina washcoating (left) and a cordierite monolith channel with alumina washcoating (right). Yellow circles point out EDS analysis spots

The presence of γ-alumina was confirmed using energy dispersive X-ray spectrometry (EDS). Typical zones analysed are circles in yellow in the picture on the right of Figure 12. It confirmed the mass increase observed by gravimetry and ensured the good deposition of the porous alumina phase with a high specific surface area.

This technique was then applied to impregnated catalysts to control the possible presence of trace of remaining chlorine. This element could be retrieved subsequently to the impregnation of the washcoated carriers with a precursor salt containing chlorine, both for rhodium and platinum (hexachloroplatinic acid, and rhodium chloride, respectively), to explain the lack of catalytic activity or the need for pre-activation steps of the catalysts, as assumed at the end of section 3.2. Several points were focused on the catalyst to check whether there were any preferential sites for chlorine poisoning: on the porous layer, on the carrier support material (cordierite) and on the active phase sites. Resulst of such tests are depicted in Figure 13.

DOI: 10.13009/EUCASS2019-357

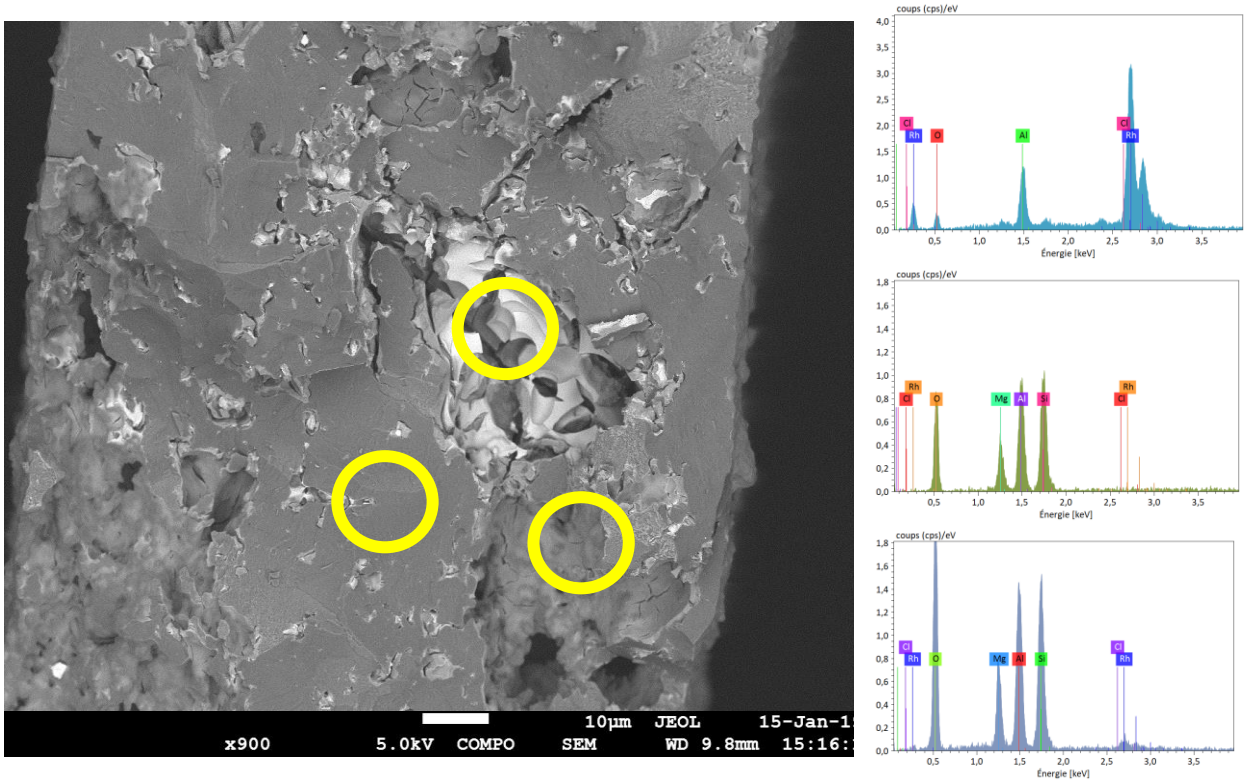

Figure 13: SEM cliché obtained from a 15 % rhodium-based catalyst (left picture) with EDS analyses (spectra on the right)

EDS results showed no evidence of chlorine presence on the catalyst surface. The first hypothesis assuming that remaining chlorine could poison the catalyst, thus inhibiting the catalytic reaction, is not confirmed and can be rejected.

- Transmission electron microscopy (TEM)

The metal particle (active phase) size distribution of platinum-based catalysts was determined using TEM and is presented in Figure 14. Black dots which can be seen on the TEM picture are platinum nanoparticles.

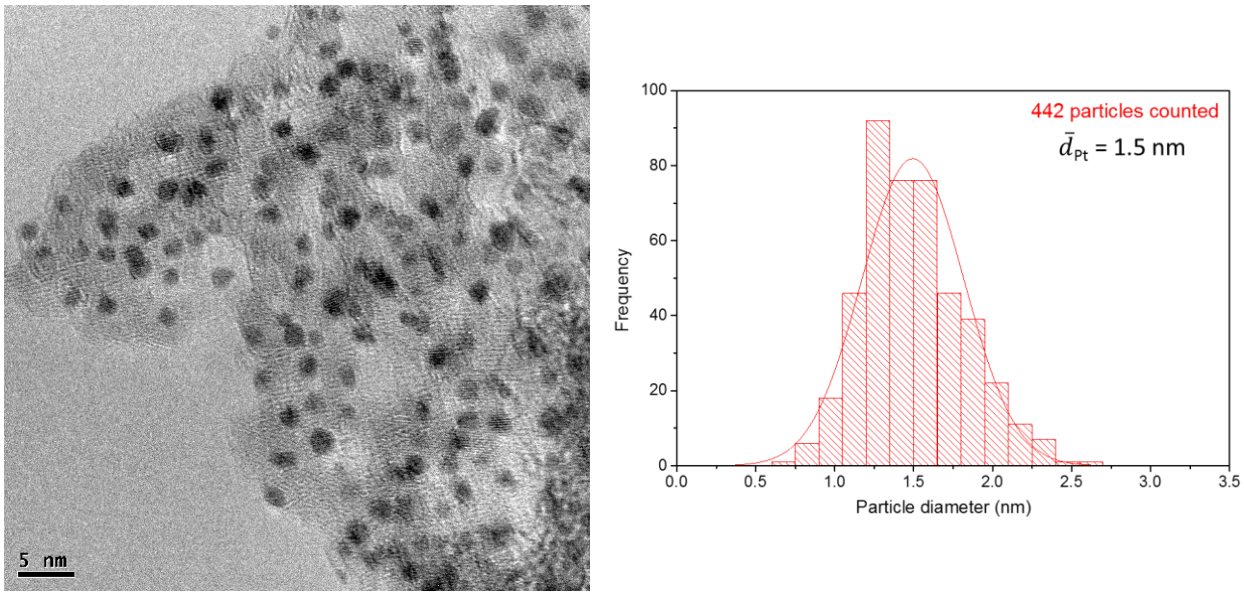

Figure 14: TEM picture of a 5 % platinum-based catalyst (left picture) and platinum size distribution (right)

DOI: 10.13009/EUCASS2019-357

The particles mean small size accounts for a good dispersion of the metal on the porous layer, which promotes the surface contact of the reactive molecules (H_2 and O_2).

- X-ray diffraction (XRD)

XRD was used to monitor crystalline phases constituting the catalysts, in particular the active phase deposition, at the desired oxidation state. The diffraction pattern recorded from a XX % Pt catalyst is shown in Figure 15.

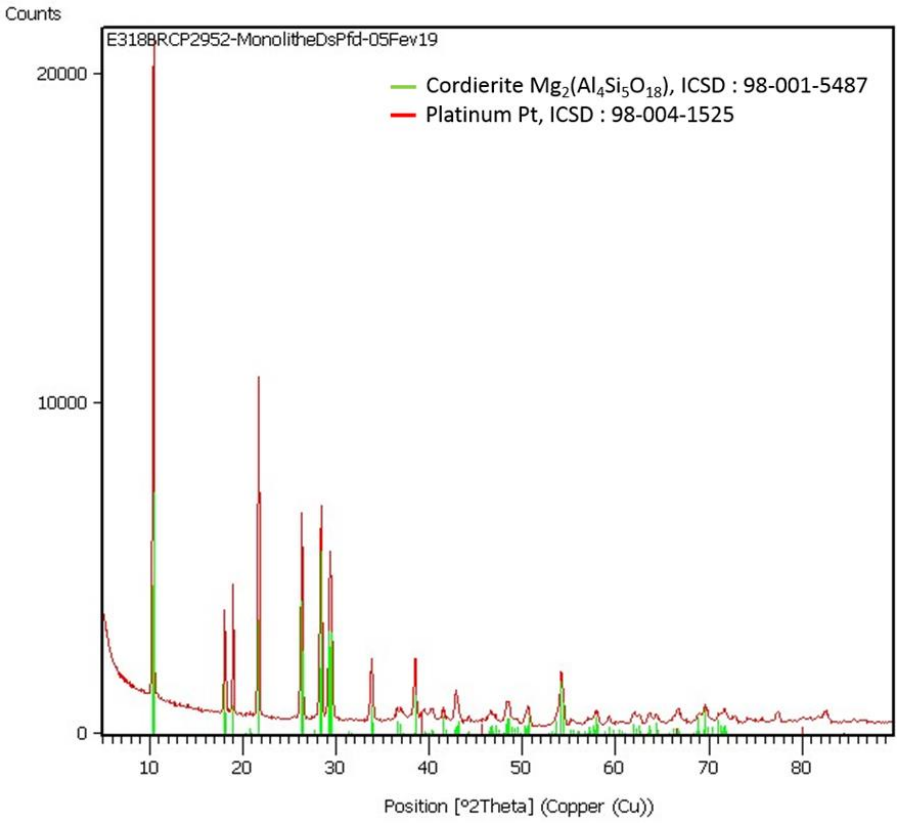

Figure 15: XRD pattern of a 5 % platinum catalyst. Green and red peaks show deviation angles of reference materials (platinum in red, cordierite in green)

The XRD pattern highlights mostly the presence of cordierite (PDF n° 98-001-5487), as well as the presence of Pt^0 (PDF n° 98-004-1525). The more intensive signals assigned to cordierite can be explained by the preparation method of the samples for XRD analysis. The catalyst was neither crushed, nor ground in fine powder. It was analysed in non-destructing conditions. The catalyst was positioned on the sample holder in such a manner that the outer cross section was aligned with the focal plane of the X ray beam. In this part of the catalyst, the washcoat layer thickness and active phase nanoparticles are in lower quantities than inside the channels. The porous layer is amorphous and thin, whereas the platinum particle size is very small and spread throughout the surface of the porous layer which is thin (as determined by TEM) and at its quantity is weak compared to carrier. This makes its XRD signal difficult to detect.

Conclusions

The catalytic combustion of a trigas mixture (GO_2 and GH_2 in the stoichiometric ratio diluted in 85 vol. % N_2) was considered as a possible alternative to cold-gas technology. Honeycomb monolith catalysts with 600 cpsi square, straight channels were prepared. The catalysts substrates (L 20 mm; Ø 10 mm) were from cordierite, coated with porous γ-alumina onto which Pt or Rh active phase was deposited. The catalytic ignition tests performed at different initial temperatures (from -55 °C to ambient temperature) showed promising results with platinum-based catalysts. The results lead the authors to estimate a gain of specific impulse (I_{SP}) of at least 30 % compared to cold-gas propulsion. The main parameter with which the determination of catalyst performances was assessed was the Gas Hourly Space Velocity (GHSV). An optimum of this parameter was observed considering the maximum temperature reached at the reactor outlet during a combustion test. By knowing this optimum value for a given system and the flowrates that will

DOI: 10.13009/EUCASS2019-357

be used for the application, a catalytic bed dimensioning could be proposed. It will help for the catalytic bed upscaling to reach reference conditions for a SpacePlane application as close as possible.
To verify this assessment, a future dimensioning at higher scale (but still at laboratory scale) of the catalytic bed is being sought.
The catalysts have been characterized thanks to physicochemical analyses in order to find connections between catalyst performances and structural, physical and chemical properties.
Some catalysts needed a "pre-activation" step at lower flowrates to be able to initiate the combustion at higher flowrates. This means that no ignition could be observed when testing them primarily at higher flowrates. Amongst assumptions made to account for this behaviour, remaining, poisoning chlorine on the catalyst surface could be excluded from TEM-EDS analyses.
It was shown that decreasing platinum loading did not impact the performances significantly, whatever the initial temperature. This tendency needs to be confirmed as far as both ageing of the catalyst and its lifetime are concerned.

Acknowledgments

The authors gratefully acknowledge financial support from ArianeGroup, from the European Union (ERDF) and "Région Nouvelle-Aquitaine". PC is indebted to ArianeGroup and the "Association Nationale de la Recherche et de la Technologie" (ANRT) for PhD funding.

References

[1] H.E. Barber, C.H. Buell, Rocketdyne, Tridyne altitude control thruster investigation, final report, 1970, 72.
[2] K. Pedersen, V. Dorado, 2013. Tri-gas Thruster Performance Characterization, AIAA 2013-3755.
[3] G.K. Boreskov, Journal de Chimie Physique et de Physico-Chimie Biologique, 51 (1954), 759-68.
[4] V.N. Nguyen, R. Deja, International Journal of Hydrogen Energy Vol.43, Issue 36 (2018), 17520-17530.
[5] R. Amrousse, Y. Batonneau, 2010. Catalytic Combustion of Hydrogen-Oxygen Cryogenic Mixtures over Cellular Ceramic-Based Catalysts, AIAA 2010-7055.
[6] F. Rigas, P. Amyotte, Hydrogen Safety. CRC Press, 2012.
[7] F. Sadeghi, B. Tirandazi, Chemical Engineering Research and Design, 118 (2017), 21-30.
[8] A. Cybulski, J.A. Moulijn, Structured Catalysts and Reactors. 2nd edition, CRC Press, 2006.